Mathematics and Systems Science 2025, 3(3), 3811.
https://doi.org/10.54517/mss3811

Article

Mathematical modeling of HIV/AIDS transmission dynamics: Mass rape and the use of post-exposure prophylaxis (PEP)

Abdelkadir Muzey Mohammed[1,*], Habtu Alemayehu Atsbaha[1], Yohannes Yirga Kefela[1], Woldegebriel Assefa Woldegerima[1], Kiros Tedla Gebrehiwot[2]

[1] Department of Mathematics, College of Natural and Computational Sciences, Mekelle University, Mekelle 231, Ethiopia
[2] Institute of Biomedical Sciences, College of Health Science, Mekelle University, Mekelle 231, Ethiopia
*** Corresponding author:** Abdelkadir Muzey Mohammed, abdelkadir.muzey@mu.edu.et

CITATION

Mohammed AM, Atsbaha HA, Kefela YY, et al. Mathematical modeling of HIV/AIDS transmission dynamics: Mass rape and the use of post-exposure prophylaxis (PEP). Mathematics and Systems Science. 2025; 3(3): 3811. https://doi.org/10.54517/mss3811

ARTICLE INFO

Received: 10 June 2025
Revised: 20 July 2025
Accepted: 5 August 2025
Available online: 30 August 2025

Abstract: This study presents a deterministic mathematical model to investigate the transmission dynamics of HIV/AIDS, with a particular focus on mass rape as a significant driver of new infections and the mitigating effects of post-exposure prophylaxis (PEP) and antiretroviral (ARV) treatments. The model explicitly incorporates intensity of rape into the transmission framework and assesses the impact of PEP in reducing new HIV infections. Analytical results include the existence and uniqueness of positive solutions, equilibrium points, the basic reproduction number (R_0), and global stability conditions for both disease-free and endemic equilibria. Numerical simulations are performed to support and illustrate the analytical findings. The results reveal a linear relationship between the incidences of rape and R_0 while showing an inverse relationship between PEP coverage and R_0 , indicating that timely and widespread PEP administration can significantly reduce HIV transmission, especially in regions affected by sexual violence. Furthermore, the study demonstrates that combined intervention strategies involving both PEP and ARV treatments produce synergistic effects, substantially suppressing HIV transmission. These findings emphasize the importance of integrated treatment strategies over isolated interventions. Despite the substantial impact of these interventions, the model suggests that the disease remains endemic under certain conditions. By explicitly integrating conflict-related factors, particularly mass rape and treatment disruption, this model provides a novel, evidence-based framework for informing policy in humanitarian emergencies. It enables global health actors to prioritize interventions and allocate limited resources more effectively.

Keywords: HIV/AIDS; conflict related rape ; PEP: ARV; mathematical modeling; stability analysis

1. Introduction

The human immunodeficiency virus (HIV) continues to pose a serious public health challenge worldwide [1,2], with an estimated 38.4 million people currently living with the virus [3]. HIV primarily affects the immune system and, if left untreated, can progress to acquired immunodeficiency syndrome (AIDS). The primary transmission routes of HIV include unprotected sexual contact, mother-to-child transmission, sharing of contaminated needles, and transfusion of infected blood [4,5]. However, in recent decades, conflict-related sexual and gender-based violence (SGBV), particularly rape, has emerged as a significant and underexplored mode of HIV transmission, in conflict-affected regions [6–8].

The intersection of HIV transmission and SGBV is particularly alarming in regions plagued by civil unrest, where widespread rape is used as a weapon of war.

Studies show a marked increase in HIV incidence in countries undergoing armed conflict, with evidence from seven conflict-affected sub-Saharan nations indicating a sharp rise in sexual violence and HIV transmission rates [7,8]. Data from the war in Tigray, northern Ethiopia, revealed that in a community based survey; approximately 2.7 % of women who survived conflict-related sexual violence were HIV-positive [9]. Furthermore, in Rwanda, 60–80% of women raped during the 1994 genocide were estimated to be HIV-positive, compared to 13.5% in the general population [10]. The increased vulnerability of women and children during conflicts, due to displacement, weakened healthcare infrastructure, and limited access to protection further exacerbates the risk of HIV acquisition [11–14].

To mitigate the spread of HIV, major advances have been made in treatment and prevention. ARV has significantly reduced morbidity and mortality among people living with HIV [4]. Moreover, pre-exposure prophylaxis (PrEP) and PEP have emerged as crucial biomedical interventions in HIV prevention strategies. PEP, in particular, involves the intake of antiretroviral drugs for 28 days following a potential exposure, such as rape, and is most effective when initiated within 72 hours [15–17]. Nsuami and Witbooi [17] demonstrate that timely initiation of PEP significantly reduces the risk of HIV acquisition after recent possible exposure to HIV.

Despite these medical advancements, the implementation of PEP in conflict settings remains limited. Many survivors do not receive timely care due to stigma, lack of access, or disrupted healthcare systems. Integrating PEP into emergency response protocols in war-affected areas is therefore critical to curb rape-related HIV infections [16,17].

Mathematical modeling has emerged as a powerful tool to understand the complex dynamics of infectious diseases, including HIV/AIDS. These models offer a cost-effective, flexible, and scalable approach to assess transmission patterns, evaluate intervention strategies, and predict epidemic trajectories under different scenarios [17–25]. Models incorporating rape and SGBV as specific transmission pathways have been relatively limited, with most focusing on general HIV transmission dynamics. Nonetheless, a few studies have highlighted the importance of including these factors. Anema et al. [7] and Virginie et al. [8] have demonstrated the importance of including SGBV-related parameters to evaluate epidemic outcomes in conflict zones. Additionally, Baba et al. [26] and others [27] presented models highlighting how behavioral and treatment interventions can mitigate the impacts of rape-driven HIV transmission.

In this study, we extend previous models by explicitly incorporating mass rape as a transmission driver and the role of PEP as a mitigating intervention. Our compartmental epidemic model integrates key HIV dynamics with the effects of sexual violence and post-exposure treatment. This approach allows us to simulate the epidemiological consequences of conflict-related rape and assess how PEP coverage levels influence HIV incidence and prevalence.

The main aim of this paper is to investigate the potential impact of mass rape during conflict on HIV transmission dynamics and to examine the effectiveness of PEP in reducing rape-related HIV infections. By combining epidemiological data, clinical intervention strategies, and mathematical modeling, this study provides a

novel and comprehensive framework for understanding and responding to HIV epidemics in conflict settings.

2. Model description and formulation

The model we developed here is an epidemic model for the transmission dynamics of HIV-AIDS with treatment. The model incorporates some essential variables and parameters that enable the assessment of the effect of mass rape on the transmission dynamics of HIV/AIDS as well as the effect of PEP on reducing new HIV infection. The model assumptions and descriptions of the system variables and parameters are presented in the next sub sections.

2.1. Description of model variables and parameters

For our study purpose, the total population N at time t was divided into five mutually exclusive compartments: susceptible individuals $S(t)$, infected individuals with no clinical symptoms $I(t)$, infected individuals due to rape with no clinical symptoms $I_r(t)$, infected individuals with clinical symptoms $J(t)$ and a class of individuals with full-blown AIDS $A(t)$. The total population N(t) is

$$N(t) = S(t) + I(t) + I_r(t) + J(t) + A(t) \quad (1)$$

The model specifically focuses on the HIV transmission dynamics due to rape incidents by considering settings where rape is prevalent. In conflict-affected regions, mass rape is frequently used as a weapon of war, and access to healthcare is often severely disrupted due to infrastructure collapse, stigma, and population displacement. These disruptions hinder timely access to PEP and ARV, both of which are critical for preventing HIV transmission and progression.

To reflect these real-world constraints, the model incorporates variable PEP (ϕ_1) and ARV treatment rates (ϕ_2) across different scenarios. For conservative estimation under parameter uncertainty, it assumes an equal average number of sexual contacts (c) and a uniform transmission probability (β_1) for both consensual and non-consensual (rape) sexual encounters, although evidence suggests that rape carries a higher per-act transmission risk. The model also assumes equal natural birth and death rates (μ), maintaining a demographically stable population in the absence of AIDS-related mortality.

While treatment effectiveness in practice depends on adherence and timeliness, the model simplifies these dynamics by assuming that individuals receiving PEP or ARVs return to less infectious or susceptible compartments with full efficacy.

2.2. Assumptions and model formulation

The hypotheses and guiding principles of our HIV epidemic model are translated into the following core assumptions:

(A_1). Homogeneous Mixing: The population mixes homogeneously, meaning each individual has an equal probability of interacting with any other individual, regardless of demographic or geographic distinctions.

(A_2). Large Population Size: The total population size N(t) is assumed to be sufficiently large to allow deterministic modelling using continuous variables and ordinary differential equations.

(A3). Constant Natural Demographic Rates: Births and natural deaths occur at a rate μ and we assume demographic equilibrium where the birth rate equals the natural death rate.

(A_4). Recruitment rate: New individuals enter the susceptible population at a rate μΛ, maintaining the replenishment of susceptible in the system.

(A_5). Transmission Pathways: HIV is transmitted through two primary routes:

- Non-rape-related exposures: including consensual sex, needle sharing, contaminated blood, and vertical transmission.
- Rape and SGBV-related exposures: This rout reflecting the distinct progression associated with conflict-related sexual violence.

(A_6). Uniform Transmission Probability and Infectivity: Though it is well documented that Probability of transmission in SGBV is high, for conservative modeling, the same transmission rate (β_1) is assumed for all sexual exposures, removing the distinction between consensual and rape-related transmission probabilities. The symptomatic class J has a higher transmission rate β_1 with $\beta_2 > \beta_1$ reflecting greater infectivity due to higher viral load and more advanced disease stage.

(A_7). PEP and ARV Intervention:

- PEP is administered to individuals in the I_r compartment at rate ϕ_1, allowing them to return to the susceptible class if effective.
- ARV is administered to individuals in the J compartment at rate ϕ_2, allowing them to return to the asymptomatic infected class I, and reflecting treatment-induced viral suppression.

(A_8). AIDS Stage Assumption: Individuals who progress to full-blown AIDS (A) experience a high death rate δ, and their ability to transmit the virus is assumed to be negligible due to disease severity, immobility, or death.

(A_9). Constant Disease Progression:

- Disease progresses from the asymptomatic classes I and I_r to J at a constant rate of k_1 and α_1 respectively. Furthermore, from the symptomatic class J to the full-blown AIDS class A at a constant rate of k_2.
- Impact of rape during conflict: a fraction θ of new infections result from rape-related exposures, reflecting the epidemiological burden of SGBV during armed conflict.

(A_{10}). Effectiveness of PEP: PEP is assumed to be most effective when initiated within 72 hours of exposure and continued for 28 days, which is modelled by the parameter ϕ_1.

Based on the model assumptions, the above list of variables as well as parameters, the population flow diagram of the HIV epidemic model is presented in **Figure 1**.

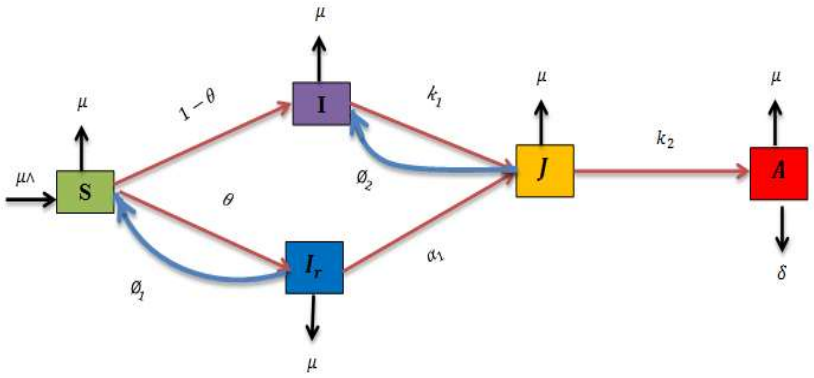

Figure 1. Flow diagram of the HIV/AIDS model with raped compartment and PEP intervention.

With an appropriate in-flow and out-flow rates of each compartment, the population flow diagram shown in **Figure 1** can be translated into HIV/AIDS epidemic model. Thus, deterministic HIV/AIDS epidemic model involving raped compartment with the use of PEP is presented using a system of DEs with non-negative initial conditions in Equation (2).

$$\left.\begin{aligned} \frac{dS}{dt} &= \mu\wedge - (\lambda+\mu)S + \emptyset_1 I_r \\ \frac{dI}{dt} &= (1-\theta)\lambda S - (k_1+\mu)I + \emptyset_2 J \\ \frac{dI_r}{dt} &= \theta\lambda S - (\alpha_1+\emptyset_1+\mu)I_r \\ \frac{dJ}{dt} &= k_1 I + \alpha_1 I_r - (k_2+\emptyset_2+\mu)J \\ \frac{dA}{dt} &= k_2 J - (\mu+\delta)A \end{aligned}\right\} \quad (2)$$

$S(0) = S_0 > 0$, $(0) = I_0 \geq 0$, $I_r(0) = I_{r0} \geq 0$, $\mathrm{J}(0) = J_0 \geq 0$ and $A(0) = A_0 \geq 0$, where $\lambda = c(\beta_1 I + \beta_1 I_r + \beta_2 J)$ is force of infection.

3. Invariant region, existence of solution and positivity of the solution

Since the model addresses changes in the human population, the variables and the parameters are expected to be positive for all $t \geq 0$. Furthermore, our system needs to be analyzed in a bounded feasible region; i.e., if the system has nonnegative initial data, then the solution of the system needs to remain positive inside the feasible region for $\forall t \geq 0$.

3.1. Invariant region

Here we show the invariant region, in which the model solution is bounded. For this purpose, we consider the following theorem.

Theorem 1. *Let* $S(0) > 0, I(0) \geq 0, I_r(0) \geq 0, J(0) \geq 0, A(0) \geq 0$ *be the initial conditions of the model system. Then, the solutions* $\{S, I, I_r, J, A\}$ *of the system are bounded* $\forall t \geq 0$.

Proof: First we considered the total human population $N = S + I + I_r + J + A$. Then, differentiating N both sides with respect to t leads to;

$$\frac{dN}{dt} = S' + I' + I_r' + J' + A' \tag{3}$$

Combining (2) and (3), we can get $\frac{dN}{dt} \leq \mu\wedge\ - \mu N - \delta A$.

In the absence of mortality due to AIDS becomes

$$\frac{dN}{dt} \leq \mu\wedge\ - \mu N \tag{4}$$

Equivalently this inequality can be expressed as $\frac{dN}{dt} + \mu N \leq \mu\wedge$. Upon solving the inequality, the general solution is given as $N(t) \leq \wedge + Ce^{-\mu t}$, but, $N(0)$ is the initial values of the respective variable $N(t) = N(0)$ at $t = 0$. Thus, the particular solution is expressed as

$$N(t) \leq \wedge + [N(0) - \wedge]e^{-\mu t} \tag{5}$$

Moreover, $N(t) \to \wedge$ as $t \to \infty$. That is, the total population size $N(t)$ takes off from the value $N(0)$at the initial time $t\ =\ 0$ and ends up with the bounded value $\wedge$ as the time $t \to \infty$. Therefore, it can be concluded that $N(t)$is bounded as $0 \leq N(t) \leq \wedge$ .Thus, the feasible solution set of the system of equations for the model enters and remains in the region:

$$\Gamma = \{(S, I, I_r, J, A) \in R_+^5 : N(t) \leq \wedge\} \tag{6}$$

Therefore, the epidemic model (2) is epidemiologically and mathematically well posed. Hence, it suffices to study the dynamics of the basic model in the region Γ.

3.2. Existence of the solution

Theorem 2. *(Existence) Solutions of the model (2) together with the initial conditions* $S(0) > 0$, $I(0) \geq 0$, $I_r(0) \geq 0$, $J(0) \geq 0$, $A(0) \geq 0$ *exist in* R_+^5*; i.e, the model variables* $S(t), I(t), I_r(t), J(t)$ *and* $A(t)$ *exist for all* t *and will remain in* R_+^5.

Proof: The right hand sides of the model equations in (2) can be described as function of $f_i(S, I, I_r, J, A) = f_i$, where $i = 1,2,3,4,5$.

$$\left.\begin{array}{c} f_1 = \mu\wedge - \ (\lambda + \mu)S + \emptyset_1 I_r \\ f_2 = (1 - \theta)\lambda S - (k_1 + \mu)I + \emptyset_2 J \\ f_3 = \theta\lambda S - (\alpha_1 + \emptyset_1 + \mu)I_r \\ f_4 = k_1 I + \alpha_1 I_r - (k_2 + \emptyset_2 + \mu\ )J \\ f_5 = k_2 J - (\mu + \delta)A \end{array}\right\} \tag{7}$$

Let Γ denote the region $\Gamma = \{(S, I, I_r, J, A) \in R_+^5 : N(t) \leq \wedge\}$. Then according the Derrick and Groosman theorem cited in [28], the DEs in (2) have a unique solution if $\partial f_i / \partial x_i$, $i = 1,2,3,4,5$, are continuous and bounded in Γ. Here, $x_1 = S$, $x_2 = I$, $x_3 = I_r$, $x_4 = J$ and $x_5 = A$ and $\lambda = c(\beta_1 I + \beta_1 I_r + \beta_2 J)$.

Table 1 bellow summarizes the continuity and boundedness of the system:

Table1. Continuity and boundedness of the mode derivatives.

$\frac{\partial f_1}{\partial S} = \lvert-(\lambda+\mu)\rvert \leq \wedge + \mu < \infty$	$\frac{\partial f_3}{\partial S} = \lvert\theta\lambda\rvert < \infty$
$\frac{\partial f_1}{\partial I} = \lvert-c\beta_1 S\rvert < \infty$	$\frac{\partial f_3}{\partial I} = \lvert c\theta\beta_1 S\rvert < \infty$
$\frac{\partial f_1}{\partial I_r} = \lvert-c\beta_1 S + \emptyset_1\rvert < \infty$	$\frac{\partial f_3}{\partial I_r} = \lvert c\theta\beta_1 S - (\alpha_1 + \emptyset_1 + \mu)\rvert < \infty$
$\frac{\partial f_1}{\partial J} = \lvert-c\beta_2 S\rvert < \infty$	$\frac{\partial f_3}{\partial J} = \lvert c\theta\beta_2 S\rvert < \infty$
$\frac{\partial f_1}{\partial A} = 0 < \infty$	$\frac{\partial f_3}{\partial A} = 0 < \infty$
$\frac{\partial f_2}{\partial S} = \lvert(1-\theta)\lambda\rvert < \infty$	$\frac{\partial f_4}{\partial S} = 0 < \infty$
$\frac{\partial f_2}{\partial I} = \lvert c(1-\theta)\beta_1 S - (k_1+\mu)\rvert < \infty$	$\frac{\partial f_4}{\partial I} = \lvert k_1\rvert < \infty$
$\frac{\partial f_2}{\partial I_r} = \lvert c(1-\theta)\beta_1 S\rvert < \infty$	$\frac{\partial f_4}{\partial I_r} = \lvert\alpha_1\rvert < \infty$
$\frac{\partial f_2}{\partial J} = \lvert c(1-\theta)\beta_2 S + \emptyset_2\rvert < \infty$	$\frac{\partial f_4}{\partial J} = \lvert-(k_2 + \emptyset_2 + \mu\rvert < \infty$
$\frac{\partial f_2}{\partial A} = 0 < \infty$	$\frac{\partial f_4}{\partial A} = 0 < \infty$
$\frac{\partial f_5}{\partial S} = 0 < \infty$	$\frac{\partial f_5}{\partial J} = \lvert k_2\rvert < \infty$
$\frac{\partial f_5}{\partial I} = 0 < \infty$	$\frac{\partial f_5}{\partial A} = \lvert-(\mu+\delta)\rvert < \infty$
$\frac{\partial f_5}{\partial I_r} = 0 < \infty$	

Thus, all the partial derivatives $\partial f_i / \partial x_i$,$i =$ 1,2,3,4,5 exist, continuous and bounded in Γ. Therefore, by Derrick and Groosman theorem, a unique solution for the model equations in (2) exists.

3.3. Positivity of the solution

Assuming the initial condition of the system of the DEs in the model system (2) to be nonnegative, now we show that the solution of this system of DEs is also positive.

Theorem 3. ***Let*** $\Gamma = \{(S, I, I_r, J, A) \in R_+^5 : S(0) > 0$ **,** $I(0) \geq 0$, $I_r(0) \geq 0$ **,** $J(0) \geq 0, A(0) \geq 0\}$***; then the solutions for*** $\{S, I, I_r, J, A\}$***are positive for all*** $t \geq 0$.

Proof: Positivity is verified separately for each of the model $S(t), I(t), I_r(t), J(t)$ and $A(t)$.

Positivity of S(t): The DE corresponding to is given by $\frac{dS}{dt} = \mu\wedge - (\lambda+\mu)S + \emptyset_1 I_r$. After eliminating the positive terms which appear on the right hand side of the equation, the equation can be expressed as $\frac{dS}{dt} \geq -(\lambda+\mu)S$

where $\lambda = c(\beta_1 I + \beta_1 I_r + \beta_2 J)$. Using integration by method of variable separation, the solution of the earlier differential inequality can be given as $S(t) \geq S_0 e^{-(\lambda+\mu)t}$. We also know that an exponential function is always non–negative irrespective of the sign of the exponent. Thus, $S(t) \geq 0$ for all t follows from the as the non-negativity of the exponential function $e^{-(\lambda+\mu)t}$.

Positivity of I(t): The DE associated with $I(t)$ is $\frac{dI}{dt} = (1-\theta)\lambda S - (k_1 + \mu)I + \emptyset_2 J$. This can also be expressed as $\frac{dI}{dt} \geq -(k_1 + \mu)I$ after eliminating the positive terms. Using integration by method of variable separation, the solution of the differential inequality can be written as $I(t) \geq I_0 e^{-(k_1+\mu)t}$. Furthermore, the non-negativity of the exponential function $e^{-(k_1+\mu)t}$ implies $I(t) \geq 0\ \forall t$.

Positivity of $\mathbf{I_r}$(t): The DE corresponding with $I_r(t)$ is $\frac{dI_r}{dt} = \theta\lambda S - (\alpha_1 + \emptyset_1 + \mu)I_r$. After eliminating the positive terms, the DE can be written as $\frac{dI_r}{dt} \geq -(\alpha_1 + \emptyset_1 + \mu)I_r$. Integrating the differential inequality after separation of variables give the solution $I_r(t) \geq (t)\ I_{r0} e^{-(\alpha_1+\emptyset_1+\mu)t}$. Since $e^{-(\alpha_1+\emptyset_1+\mu)t}$ is always non-negative; and hence $I_r(t) \geq 0\ \forall t$.

Positivity of J(t): The DE associated with $J(t)$is given by $\frac{dJ}{dt} = k_1 I + \alpha_1 I_r - (k_2 + \emptyset_2 + \mu\ )J$. After eliminating the positive terms, the DE can be reduced to $\frac{dJ}{dt} \geq -(k_2 + \emptyset_2 + \mu\ )J$. Integrating the differential inequality also gives $J(t) \geq J_0 e^{-(k_2+\emptyset_2+\mu)\ t}$. However, the exponential expression $e^{-(k_2+\emptyset_2+\mu)\ t}$is always non negative. The positivity of the solution for $J(t)\ \forall t$, therefore, follows from the positivity of $J(t) \geq J_0 e^{-(k_2+\emptyset_2+\mu)\ t}$.

Positivity of A(t) : The DE corresponding with $A(t)$ is $\frac{dA}{dt} = k_2 J - (\mu + \delta)A$. Eliminating the positive term $k_2 J$ from the DE leads to the differential inequality $\frac{dA}{dt} \geq -(\mu + \delta)A$. Integrating the differential inequality also gives $A(t) \geq A_0 e^{-(\delta+\mu)\ t}$. In a similar fashion, the positivity of $A(t)$ for all t follows from the positivity of $A(t) \geq A_0 e^{-(\delta+\mu)\ t}$.

Hence, it can be concluded that the model variables $S(t), I(t), I_r(t), J(t)$ and $A(t)$ representing population sizes of different HIV infection level are positive and will remain in R_+^5 for all t.

4. Reproduction number and Equilibrium points

To understand the behaviour of the system (2) as well as the conditions under which the disease may be eradicated or become endemic, the basic reproduction number and equilibrium points are epidemiologically important; for instance see [17–29]. In line with the methodological framework of Lu and colleagues [30], who incorporated multiple infection pathways into reproduction number and equilibrium analyses, our HIV model similarly integrates both conventional (non - rape) transmission routes and conflict-driven rape exposure into the next-generation matrix, thereby capturing how these parallel pathways jointly shape the threshold condition and long-term stability of the endemic.

4.1. Reproduction number

Epidemiologically, the reproduction number reflects the number of secondary cases that one infectious individual will produce in a population consisting only of susceptible individuals. Different approaches, including Jacobian and next generation matrix approaches can be employed to compute the reproduction number of a given model. In this work, we used the next generation matrix method. To calculate the basic reproduction number via the next generation matrix, we take the infectious compartments to be I, I_r and J. With these considerations, now let $F_i(x) = \begin{pmatrix} c(1-\theta)(\beta_1 I + \beta_1 I_r + \beta_2 J)S \\ \theta(\beta_1 I + \beta_1 I_r + \beta_2 J)S \\ 0 \end{pmatrix}$, and $V_i(x) = \begin{pmatrix} (k_1+\mu)I - \emptyset_2 J \\ (\alpha_1 + \emptyset_1 + \mu)I_r \\ -k_1 I - \alpha_1 I_r + (k_2 + \emptyset_2 + \mu)J \end{pmatrix}$, then system (2) is written as

$$x' = F - V \tag{8}$$

where $x = [I,\ I_r,\ J]^{\,t}$; $F = \left(\frac{\partial F_i}{\partial x_j}\right)$ is the rate of appearance of new infections in compartment $I, I_r, and\ J$; $V = \left(\frac{\partial V_i}{\partial x_j}\right)$ is the rate at which the population in each compartment changes due to compartmental transfers as a result of status changes caused by disease dynamics.

Consequently, we have $F = \begin{pmatrix} c(1-\theta)\beta_1 S & c(1-\theta)\beta_1 S & c(1-\theta)S\beta_2 S) \\ c\theta\beta_1 S & c\theta\beta_1 S & c\theta\beta_2 S \\ 0 & 0 & 0 \end{pmatrix}$ and $V = \begin{pmatrix} k_1+\mu & 0 & -\emptyset_2 \\ 0 & \alpha_1+\emptyset_1+\mu & 0 \\ -k_1 & -\alpha_1 & k_2+\emptyset_2+\mu \end{pmatrix}$.

The matrix F computed at the disease-free equilibrium $\in_0 = (\wedge, 0, 0, 0)$ is $F(\in_0) = \begin{pmatrix} c(1-\theta)\beta_1\wedge & c(1-\theta)\beta_1\wedge & c(1-\theta)S\beta_2\wedge) \\ c\theta\beta_1\wedge & c\theta\beta_1\wedge & c\theta\beta_2\wedge \\ 0 & 0 & 0 \end{pmatrix}$.

The matrix F is a nonnegative matrix of rank one for $0 \le \theta \le 1$, whereas V is a non-singular M-matrix and a nonnegative matrix has a real eigenvalue equal to its spectral radius [31]. According to Van den Driessche and Watmough [29], the reproduction number R_0 of our model is the spectral radius of the matrix FV^{-1} and the spectral radius of the matrix FV^{-1} is defined as the maximum modulus of its eigenvalues and is given by $\rho(FV^{-1})$. Thus, to determine the spectral radius of FV^{-1}, we first represent the inverse of V by the following matrix:

$$V^{-1} = \frac{1}{\det(V)} \begin{pmatrix} v_{12} & v_{12} & v_{13} \\ v_{21} & v_{22} & v_{23} \\ v_{31} & v_{32} & v_{33} \end{pmatrix}$$

where $v_{11} = (\alpha_1 + \emptyset_1 + \mu)(k_2 + \emptyset_2 + \mu)$, $v_{12} = \alpha_1\emptyset_2$, $v_{13} = \emptyset_1(\alpha_1 + \emptyset_1 + \mu)$; $v_{21} = 0$, $v_{22} = (k_1+\mu)(k_2+\emptyset_2+\mu) - k_1\emptyset_2$, $v_{23} = 0$; $v_{31} = k_1(\alpha_1+\emptyset_1+\mu)$, $v_{32} = \alpha_1(k_1+\mu)$, $v_{33} = (k_1+\mu)(\alpha_1+\emptyset_1+\mu)$ and

$$\det(V) = \begin{vmatrix} k_1+\mu & 0 & -\emptyset_2 \\ 0 & \alpha_1+\emptyset_1+\mu & 0 \\ -k_1 & -\alpha_1 & k_2+\emptyset_2+\mu \end{vmatrix} \tag{9}$$

$$= (\alpha_1 + \emptyset_1 + \mu)[\mu(k_2 + \emptyset_2 + \mu) + k_1(k_2 + \mu)]$$

Thus, the next generation matrix for the model (2) is

$$FV^{-1} = \begin{pmatrix} A_{11} & A_{12} & A_{13} \\ A_{21} & A_{22} & A_{33} \\ A_{31} & A_{32} & A_{33} \end{pmatrix}$$

where,

$$A_{11} = \frac{c(1-\theta)\wedge}{(\alpha_1 + \emptyset_1 + \mu)}\left[\frac{\beta_1(\alpha_1 + \emptyset_1 + \mu)(k_2 + \emptyset_2 + \mu)}{\mu(k_2 + \emptyset_2 + \mu) + k_1(k_2 + \mu)} + \frac{\beta_2 k_1(\alpha_1 + \emptyset_1 + \mu)}{\mu(k_2 + \emptyset_2 + \mu) + k_1(k_2 + \mu)}\right]$$

$$A_{12} = \frac{c(1-\theta)\wedge}{(\alpha_1 + \emptyset_1 + \mu)}\left[\frac{\beta_1(k_1 + \mu)(k_2 + \emptyset_2 + \mu)}{\mu(k_2 + \emptyset_2 + \mu) + k_1(k_2 + \mu)} + \frac{\beta_1[\alpha_1\emptyset_2 - k_1\emptyset_2]}{\mu(k_2 + \emptyset_2 + \mu) + k_1(k_2 + \mu)} + \frac{\beta_2\alpha_1(k_1 + \mu)}{\mu(k_2 + \emptyset_2 + \mu) + k_1(k_2 + \mu)}\right]$$

$$A_{13} = \frac{c(1-\theta)\wedge}{(\alpha_1 + \emptyset_1 + \mu)}\left[\frac{\beta_1\emptyset_1(\alpha_1 + \emptyset_1 + \mu)}{\mu(k_2 + \emptyset_2 + \mu) + k_1(k_2 + \mu)} + \frac{\beta_2(k_1 + \mu)(\alpha_1 + \emptyset_1 + \mu)}{\mu(k_2 + \emptyset_2 + \mu) + k_1(k_2 + \mu)}\right]$$

$$A_{21} = \frac{c\theta\wedge}{(\alpha_1 + \emptyset_1 + \mu)}\left[\frac{\beta_1(\alpha_1 + \emptyset_1 + \mu)(k_2 + \emptyset_2 + \mu)}{\mu(k_2 + \emptyset_2 + \mu) + k_1(k_2 + \mu)} + \frac{\beta_2 k_1(\alpha_1 + \emptyset_1 + \mu)}{\mu(k_2 + \emptyset_2 + \mu) + k_1(k_2 + \mu)}\right]$$

$$A_{22} = \frac{c\theta\wedge}{(\alpha_1 + \emptyset_1 + \mu)}\left[\frac{\beta_1(k_1 + \mu)(k_2 + \emptyset_2 + \mu)}{\mu(k_2 + \emptyset_2 + \mu) + k_1(k_2 + \mu)} + \frac{\beta_1[\alpha_1\emptyset_2 - k_1\emptyset_2]}{\mu(k_2 + \emptyset_2 + \mu) + k_1(k_2 + \mu)} + \frac{\beta_2\alpha_1(k_1 + \mu)}{\mu(k_2 + \emptyset_2 + \mu) + k_1(k_2 + \mu)}\right]$$

$$A_{23} = \frac{c\theta\wedge}{(\alpha_1 + \emptyset_1 + \mu)}\left[\frac{\beta_1\emptyset_1(\alpha_1 + \emptyset_1 + \mu)}{\mu(k_2 + \emptyset_2 + \mu) + k_1(k_2 + \mu)} + \frac{\beta_2(k_1 + \mu)(\alpha_1 + \emptyset_1 + \mu)}{\mu(k_2 + \emptyset_2 + \mu) + k_1(k_2 + \mu)}\right]$$

$$A_{31} = A_{32} = A_{33} = 0$$

Since matrix F has rank 1, the spectral radius $\rho(FV^{-1})$ is equal to the trace of matrix FV^{-1}; i.e., $\rho(FV^{-1}) = tr(FV^{-1}) = R_0 = A_{11} + A_{22} + A_{33}$.

Thus, the reproduction number is given by

$$R_0 = \frac{c(1-\theta)\wedge\beta_1(\alpha_1 + \emptyset_1 + \mu)(k_2 + \emptyset_2 + \mu)}{(\alpha_1 + \emptyset_1 + \mu)[\mu(k_2 + \emptyset_2 + \mu) + k_1(k_2 + \mu)]} + \frac{c(1-\theta)\wedge\beta_2 k_1(\alpha_1 + \emptyset_1 + \mu)}{(\alpha_1 + \emptyset_1 + \mu)[\mu(k_2 + \emptyset_2 + \mu) + k_1(k_2 + \mu)]} + \tag{10}$$

$$+\frac{c\theta\wedge\beta_1 S[\alpha_1\emptyset_2+(k_1+\mu)(k_2+\emptyset_2+\mu)-k_1\emptyset_2]}{(\alpha_1+\emptyset_1+\mu)[\mu(k_2+\emptyset_2+\mu)+k_1(k_2+\mu)]}$$

$$+\frac{c\theta\beta_2\wedge\alpha_1(k_1+\mu)}{(\alpha_1+\emptyset_1+\mu)[\mu(k_2+\emptyset_2+\mu)+k_1(k_2+\mu)]}$$

4.2. Equilibrium points

The two epidemiologically important equilibrium points are the disease-free and endemic equilibrium points. The disease-free equilibrium point $\in_o$ is an equilibrium point with no infectious individuals, and in our case, it is also a rape-free equilibrium point. On the other hand, the endemic equilibrium point $\in^*$ is a point at which the disease persists in the population. The equilibrium points of the model system (2) are computed from the equilibrium Equation (11).

$$\left.\begin{array}{c}\mu\wedge-(\lambda+\mu)S+\emptyset_1 I_r=0\\(1-\theta)\lambda S-(k_1+\mu)I+\emptyset_2 J=0\\\theta\lambda S-(\alpha_1+\emptyset_1+\mu)I_r=0\\k_1 I+\alpha_1 I_r-(k_2+\emptyset_2+\mu)J=0\\k_2 J-(\mu+\delta)A=0\end{array}\right\} \tag{11}$$

The disease-free equilibrium point $\in_o$ is obtained by setting $I=I_r=J=A=0$. Solving (4.1) at these values yields $\in_o=(S^*,0,0,0)$, where $S^*=\wedge$.

The endemic equilibrium point $\in^*=(S^*, I^*, {I^*}_r, J^*, A^*)$ is also obtained by solving the equilibrium equations in (11) for $S\neq 0$,

$$\left.\begin{array}{c}S^*=\frac{\lambda_1[(k_1+\mu)\lambda_2-k_1\emptyset_2]}{c(1-\theta)[\beta_1\lambda_2\lambda_2+\beta_2 k_1\lambda_1]+c\ \ [\beta_1((\alpha_1-k_1)\emptyset_2+(k_1+\mu)\lambda_2)+\beta_2\alpha_1(k_1+\mu)]}\\I^*=\frac{\mu\wedge[(1-\theta)\lambda_1\lambda_2+\theta\alpha_1\emptyset_2]}{(\lambda_1-\theta\emptyset_1)[\lambda_2(k_1+\mu)-k_1\emptyset_2]}\left(1-\frac{1}{R_0}\right)\\{I^*}_r=\frac{\theta\mu\wedge}{\lambda_1-\theta\emptyset_1}\left(1-\frac{1}{R_0}\right)\\J^*=\frac{\mu\wedge}{\lambda_2(\lambda_1-\theta\emptyset_1)}\left[\frac{k_1\left((1-\theta)\lambda_1\lambda_2+\theta\alpha_1\emptyset_2\right)+\alpha_1\theta((k_1+\mu)-k_1\emptyset_2}{\lambda_2(k_1+\mu)-k_1\emptyset_2}\right]\left(1-\frac{1}{R_0}\right)\\A^*=\frac{k_2\mu\wedge}{\lambda_2(\lambda_1-\theta\emptyset_1)(\mu+\delta)}\left[\frac{k_1\left((1-\theta)\lambda_1\lambda_2+\theta\alpha_1\emptyset_2\right)+\alpha_1\theta((k_1+\mu)-k_1\emptyset_2}{\lambda_2(k_1+\mu)-k_1\emptyset_2}\right]\left(1-\frac{1}{R_0}\right)\end{array}\right\} \tag{12}$$

where $\lambda_1=\alpha_1+\emptyset_1+\mu$ and $\lambda_2=k_2+\emptyset_2+\mu$.

5. Global stability

In this section, we study the behaviour of a solution that starts at any point in the feasible region Γ as time $t\to\infty$. We now use the Lyapunov method to prove the global stability of the equilibrium points for system (2). Thus, we approach the problem by constructing a Lyapunov function considering the first four variables S, I, I_r and J.

5.1. Global stability of the disease-free equilibrium

Theorem 4. *The disease free equilibrium point* $\in_{\mathbf{0}}$ *of the system (2) is locally asymptotically stable if* $\boldsymbol{R_0<1}$ *and unstable if* $\boldsymbol{R_0>1}$.

Proof. To prove the global asymptotic stability of the DFE we use the method of Lyapunov function. Systematically, we define a Lyapunov function V such that:

$$V(S, I, I_r, J) = A_1(\wedge - S) + A_2 I + A_3 I_r + A_4 J \tag{13}$$

By direct calculating the derivative of V in equation (13),we have

$$\frac{dV}{dt} = -A_1 S' + A_2 I' + A_3 I'_r + A_4 J' \tag{14}$$

Substituting $S', I', I'_r$and $J'$from (2) in to (14) also give

$$\frac{dV}{dt} = -A_1[\mu\wedge - (\lambda + \mu)S + \emptyset_1 I_r] + A_2[(1-\theta)\lambda S - (k_1 + \mu)I + \emptyset_2 J] + A_3[\theta\lambda S - (\alpha_1 + \emptyset_1 + \mu)I_r] + A_4[k_1 I + \alpha_1 I_r - (k_2 + \emptyset_2 + \mu)J] \tag{15}$$

$$\frac{dV}{dt} = -A_1\mu(\wedge - S) + A_1\lambda S + A_1\lambda S - \emptyset_1 I_r + A_1\lambda S - A_1\theta\lambda S - A_1(k_1 + \mu)I + A_1\emptyset J + A_1\theta\lambda S - A_1(\alpha_1 + \emptyset_1 + \mu)I_r + A_4[k_1 I + \alpha_1 I_r - (k_2 + \emptyset + \mu)J]$$

$$= -A_1\mu(\wedge - S) + A_1\lambda S + A_1\lambda S - \emptyset_1 I_r + A_1\lambda S - A_1(k_1 + \mu)I + A_1\emptyset J - A_1(\alpha_1 + \emptyset_1 + \mu)I_r + A_4[k_1 I + \alpha_1 I_r - (k_2 + \emptyset + \mu)J] < -A_1\mu(\wedge - S) + A_1\lambda\wedge - \emptyset_1 I_r + A_1\lambda\wedge - A_1(k_1 + \mu)I + A_1\emptyset J \tag{16}$$

$$A_1 = -A_1(\alpha_1 + \emptyset_1 + \mu)I_r + A_4[k_1 I + \alpha_1 I_r - (k_2 + \emptyset + \mu)J]$$

$A_2 = A_3$, (15) is reduced to

The condition $R_0 < 1$ leads to $c\beta_1\wedge < k_1 + \mu$, $c\beta_1\wedge < \alpha_1 + \emptyset_1 + \mu$ and $c\beta_1\wedge < k_2 + \emptyset_2 + \mu$.

Thus, Equation (16) can also be written as

$$A_1\lambda S - A_1(k_1 + \mu)I - A_1(\alpha_1 + \emptyset_1 + \mu)I_r < D\,(R_0 - 1)[c(\beta_1 I + \beta_1 I_r + \beta_2 J] \tag{17}$$

where $D = (\alpha_1 + \emptyset_1 + \mu)[\mu(k_2 + \emptyset_2 + \mu) + k_1(k_2 + \mu)]$.

Again $R_0 < 1$ allows to find sufficiently small positive numbers A_1 and A_4 such that

$$A_1 < \frac{-D\,(R_0 - 1)c\beta_2}{c\beta_2\wedge + \emptyset_2} \text{ and } A_4 < \frac{D\,(R_0 - 1)c\beta_1}{k_1}\left[\frac{c\beta_2\wedge}{c\beta_2\wedge + \emptyset_2} - 1\right] \tag{18}$$

Combination of (16 –18) gives

$$\frac{dV}{dt} < -A_1\mu(\wedge - S) + [A_1 c\beta_1\wedge + A_4 k_1 + D\,(R_0 - 1)c\beta_1]I + [A_1 c\beta_1\wedge + A_4 k_1 + D\,(R_0 - 1)c\beta_1]I_r + [A_1 c\beta_2\wedge + A_1\emptyset_2 J k_1 + D\,(R_0 - 1)c\beta_2]J - A_1\emptyset_1 I_r < 0 \tag{19}$$

So $\frac{dV}{dt} < 0$ if $R_0 < 1$. Furthermore, $\frac{dV}{dt} = 0$ if $S = \wedge, I = 0, I_r = 0$ and $J = 0$).

From this we see that, $\in_o = (S^*, 0,0,0)$ where $S^* = \wedge$ is the only singleton in $\left\{(S^*, 0, 0, 0) \in \Gamma : \frac{dV}{dt} = 0\right\}$.

Therefore, by LaSalle's invariance principle (LaSalle's, 1976), the DFE is globally asymptotically stable in Γ if $R_0 < 0$.

5.2. Global stability of the endemic equilibrium point

Theorem 5. *If* $R_0 > 1$*, the endemic equilibrium* $\in^*$ *of the model (2) is*

globally asymptotically stable.

Proof: To prove the global asymptotic stability of the endemic equilibrium we use the method of Lyapunov functions. Define

$$V(S^*, I^*, I^*_r, J^*, A^*) = \left(S - S^* - S^* ln\frac{S}{S^*}\right) + \left(I - I^* - I^* ln\frac{I}{I^*}\right) + \left(I_r - I^*_r - I^*_r ln\frac{I_r}{I^*_r}\right) + \left(J - j^* - J^* ln\frac{J}{j^*}\right) \tag{20}$$

Using computation of the derivative of V along the solution of system 2 we have,

$$\frac{dV}{dt} = \left(1 - \frac{S^*}{S}\right)S' + A_1\left(1 - \frac{I^*}{I}\right)I' + A_2\left(1 - \frac{I_r{}^*}{I_r}\right)I_r{}' + A_3(1 - \frac{J^*}{J})J' \tag{21}$$

Substituting (2) into (21) gives

$$\frac{dV}{dt} = \left(1 - \frac{S^*}{S}\right)[\mu\wedge - (\lambda + \mu)S + \emptyset_1 I_r] + \left(1 - \frac{I^*}{I}\right)[(1-\theta)\lambda S - (k_1 + \mu)I + \emptyset_2 J] + \left(1 - \frac{I_r{}^*}{I_r}\right)[\theta\lambda S - (\alpha_1 + \emptyset_1 + \mu)I_r] + (1 - \frac{J^*}{J})[k_1 I + \alpha_1 I_r - (k_2 + \emptyset_2 + \mu)J] \tag{22}$$

Collecting positive and negative terms together yields

$$\frac{dV}{dt} = \left[\mu\wedge + \lambda S^* + k_1 I^* + (\alpha_1 + \emptyset_1)I^*_r + (k_2 + \emptyset_2)J^* + \mu\prod{}^* + \theta\lambda S\frac{I^*}{I}\right] - \left[(\mu\wedge + \emptyset_1 I_r)\frac{S^*}{S} + (\lambda S + \emptyset_2)\frac{I^*}{I} + \theta\lambda S\frac{I_r{}^*}{I_r} + (k_1 I + \alpha_1 I_r)\frac{J^*}{J} + k_2 J + \mu\prod\right] \tag{23}$$

$\frac{dV}{dt} = K - Q$, where, $K = \mu\wedge + \lambda S^* + k_1 I^* + (\alpha_1 + \emptyset_1)I^*_r + (k_2 + \emptyset_2)J^* + \theta\lambda S\frac{I^*}{I} + \mu\prod{}^*, Q = (\mu\wedge + \emptyset_1 I_r)\frac{S^*}{S} + (\lambda S + \emptyset_2)\frac{I^*}{I} + \theta\lambda S\frac{I_r{}^*}{I_r} + (k_1 I + \alpha_1 I_r)\frac{J^*}{J} + k_2 J + \mu\prod, \prod{}^* = S^* + I^* + I^*_r + J^*, \prod = \mathrm{S} + \mathrm{I} + I_r + J.$

Using the equilibrium Equation (10) and $R_0 > 1$, it is possible to show $\frac{dV}{dt} \leq 0$. However, in order to show $\frac{dV}{dt} < 0$, we show $K - Q < 0$ for all $V = (S, I, I_r, J, A) \neq V(S^*, I^*, I^*_r, J^*, A^*)$. Thus, we have the following,

- $\theta\lambda S\frac{I^*}{I} - \lambda S\frac{I^*}{I} = (\theta - 1)\lambda S\frac{I^*}{I} \leq 0$ since $0 \leq \theta < 1$
- $(\alpha_1 + \emptyset_1)I^*_r - \theta\lambda S\frac{I_r{}^*}{I_r} < 0$, since $\theta\lambda S = (\alpha_1 + \emptyset_1 + \mu)I_r$
- $(k_2 + \emptyset_2)J^* - (k_1 I + \alpha_1 I_r)\frac{J^*}{J} < 0$, $k_1 I + \alpha_1 I_r = (k_2 + \emptyset_2 + \mu)J$

By similar reasoning, it can also be shown the negativity of the difference of the remaining terms. Thus, $\frac{dV}{dt} \leq 0$ for $V = (S, I, I_r, J, A) \neq V(S^*, I^*, I^*_r, J^*, A^*)$.

Furthermore, $\frac{dV}{dt} = 0$ if and only if $S = S^*, I = I^*, I_r = I^*_r$ and $J = J^*$. Therefore, the largest compact invariant set in $\left\{(S^*, I^*, I^*_r, J^*) \in \Gamma : \frac{dV}{dt} = 0\right\}$ is the singleton endemic equilibrium $\in^*$ of the model system in (2). Thus, LaSalle's invariance principle (LaSalle's, 1976) implies that $\in^*$ is globally asymptotically stable in Γ if $\mathrm{K} < \mathrm{Q}$.

6. Numerical simulation

In this section, we present numerical simulations to illustrate the analytical results of the deterministic model (2). The simulations were conducted to investigate how the trajectories of each subpopulation (S, I, I_r, J, A) and the basic reproduction number R_0 respond to different treatment rates as well as varying rates of rape over time. The numerical simulation was executed using MATLAB software using a set of meaningful values of parameters.

6.1. Treatment access scenarios

In order to make a realistic and comprehensive simulation analysis of PEP and ARV treatment interventions, we employ different treatment and rape intensity scenarios. Worst case, limited, moderate and high treatment accesses are assumed based on WHO (2022) treatment availability classification in low income and conflict affected settings as shown in **Table 2**. Most documented instances of HIV infection resulting from conflict related rape are also used as base line for our simulation.

Table 2. WHO (2022) HIV treatment access in low income and conflict setting

Treatments	Values	Scenarios			
		Worst case	**Limited**	**Moderate**	**High**
PEP	Min-Max	0	0–0.2	0.3–0.5	0.6–0.8
	Average	0	0.1	0.4	0.7
ARV	Min-Max	0	0.1–0.3	0.4–0.6	0.7–0.9
	Average	0	0.2	0.5	0.8

These scenarios assume complete collapse of health; fragile health systems with disrupted supply chains, insecurity, and lack of infrastructure; partial healthcare functionality in a health system recovering setting; more stable post conflict situations where infrastructure is relatively restored.

6.2. Numerical simulations

The change in the number of individuals in each subpopulation S, I, I_r, J and A against time both with and without PEP and ARV treatments are investigated. The first type of simulation demonstrates the trajectories of the model solution for $R_0 < 1$. The parameter values presented in **Table 3** yields $R_0 = 0.973$ when there is no PEP and ARV treatment while $R_0 = 0.826$ at $\emptyset_1 = 0.3$ and $\emptyset_2 = 0.3$ of PEP and ARV treatment rates respectively.

Table 3. Parameter values for $\boldsymbol{R_0 < 1}$

Parameter	**∧**	**c**	**β_1**	**β_2**	**α_1**	**k_1**	**k_2**	**θ**	**μ**	**δ**
Values	120	3	0.0001	0.0005	0.1	0.2	0.2	0.2	0.01	0.01

The corresponding solution curves in **Figure 2** and **Figure 3** are constructed with two different initial values 100, 70,44,56,30 and 148, 36, 2,30,54 of S, I, I_r, J and A against time. The trajectories in these indicate that the system with different initial values converges to the point (120, 0, 0, 0, 0). The subpopulations S, I, I_r, J and A tend to zero both in the presence and absence of PEP and ARV treatments. Thus, HIV invariably converges to the disease-free equilibrium, regardless of treatment availability. However, the presence of PEP and ARV accelerates the rate at which the disease fades, indicating a clear benefit of early and consistent treatment even in potentially sub-threshold epidemics.

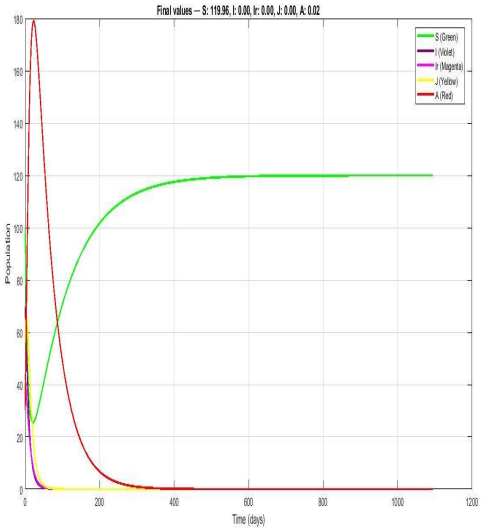

Figure 2. Model trajectories with $\emptyset_1 = 0$, $\emptyset_2 = 0$, and $\theta = 0$ for $R_0 < 1$

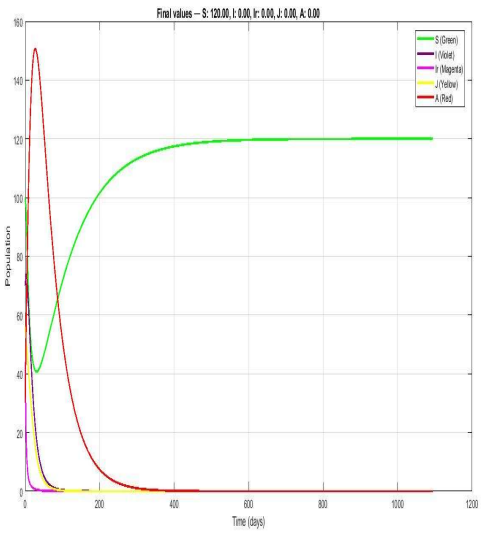

Figure 3. Model trajectories with $\emptyset_1 = 0.2$, $\emptyset_2 = 0.4$, and $\theta = 0.2$ for $R_0 < 1$

The results we obtained from the numerical simulation are consistent with the results of the analytical analysis that the disease-free equilibrium is globally stable

whenever $R_0 < 1$.This result implies that there is no transmission of disease in the population.

Some numerical simulations of the endemic solution of system (2) and its reproduction number R_0, in a general context, are performed to investigate the impact of PEP and rape on the HIV transmission dynamics. The parameter values that lead to the endemic equilibrium of our model system are presented in **Table 3**. Thus, throughout our next works on simulations, computation of the endemic equilibrium points and the computation of reproduction numbers, we are going to use these parameter values presented in Table by varying PEP treatment rate $\emptyset_1$ and the rate of rape θ.

The parameters values in **Table 4** with $\emptyset_1 = \emptyset_2 = 0$ give $R_0 = 3.922$ while $R_0 = 2.209$ whenever $\emptyset_1 = 0.1$ and $\emptyset_2 = 0.3$. To illustrate the stability of the endemic equilibrium of the model (2), model solution curves corresponding to these parameter values are constructed in in **Figures 4** and **5.**

Table 4. Parameter values for $R_0 > 0$.

Parameter	∧	**c**	**β_1**	**β_2**	**α_1**	**k_1**	**k_2**	**θ**	**μ**	**δ**
Values	300	3	0.00005	0.0001	0.01	0.3	0.05	0.2	0.01	0.01

These graphs show that the solution of the system converges to an endemic equilibrium point for $R_0 > 1$. It can be seen that as the system (2) evolves over time, the solutions with meaningful parameter values and initial conditions are convergent to an endemic equilibrium point ∈*. However, if there are PEP and ARV treatments the disease becomes less endemic, whereas in the absence of these treatments makes the disease stabilizes at more endemic level.

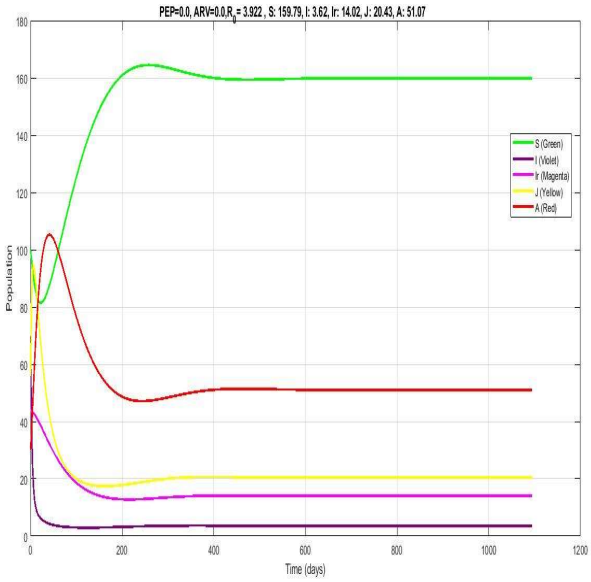

Figure 4. Trajectories with $\phi_1 = 0$, $\phi_2 = 0$ and θ = 0.2 for $R_0 > 1$

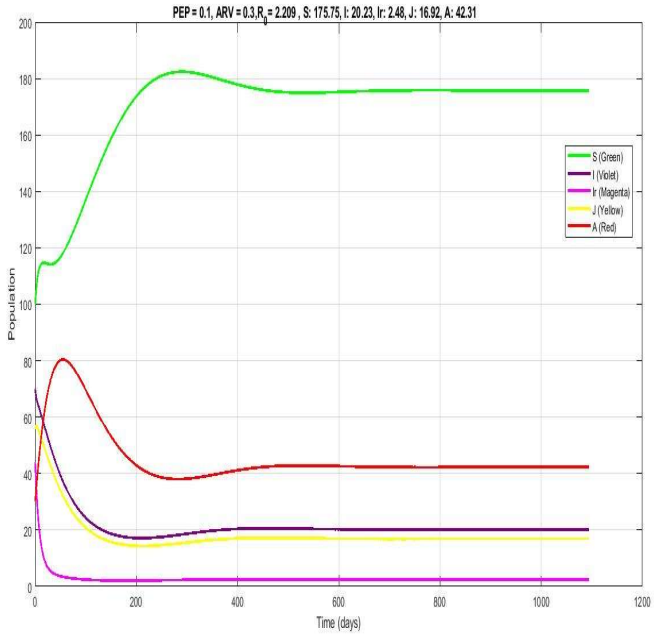

Figure 5. Trajectories $\phi_1 = 0.1$, $\phi_2 = 0.3$ and $\theta = 0.2$ for $R_0 > 1$

How the solution of the model system (2) responds to different PEP treatment rates are also investigated through simulation using different PEP scenarios with $\emptyset_1 =$ 0.2, 0.3, 0.4, and 0.8. **Figures 6** to **10** show how the subpopulations S, I, I_r, J and A of our model behave against different PEP rates with time.

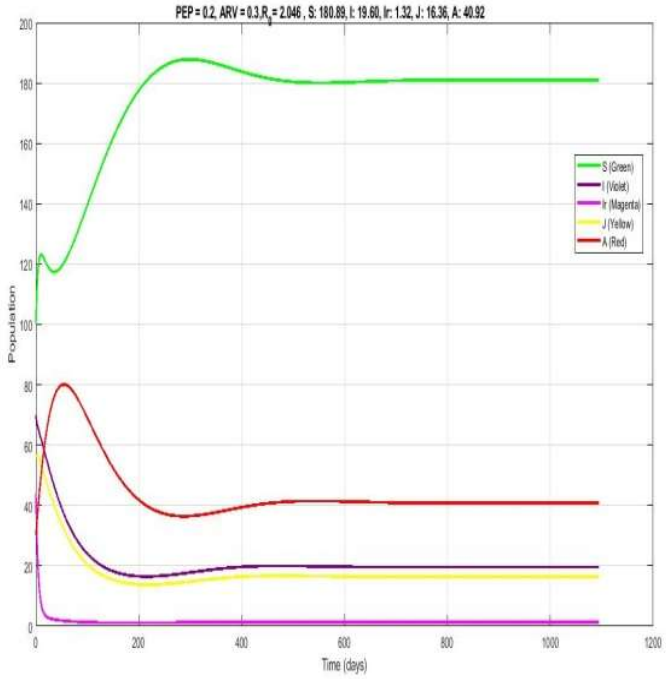

Figure 6. Trajectories with $\phi_1 = 0.2$, $\phi_2 = 0.3$ and $\theta = 0.2$ for $R_0 > 1$

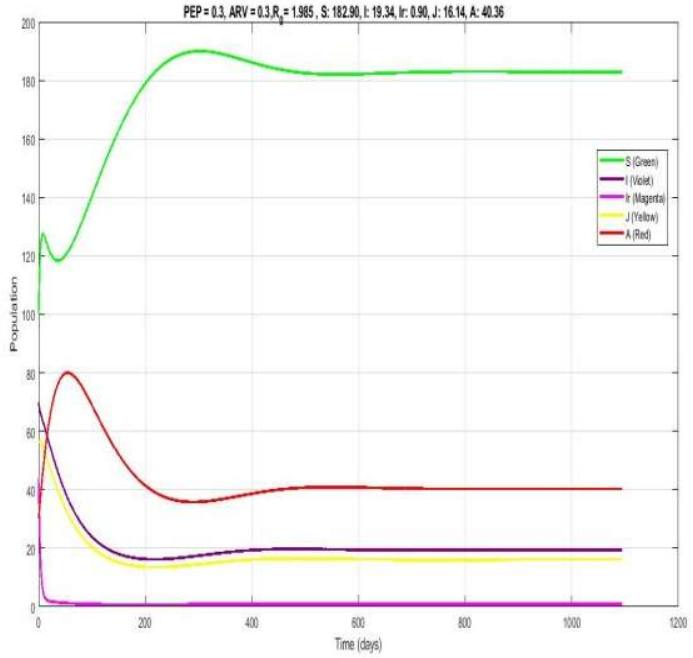

Figure 7. Trajectories with $\phi_1 = 0.3$, $\phi_2 = 0.3$ and $\theta = 0.2$ for $R_0 > 1$.

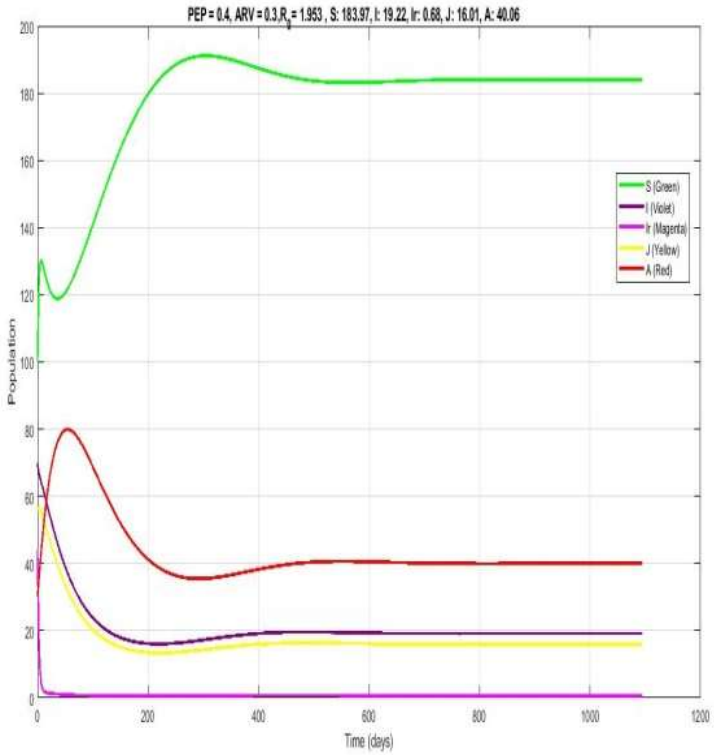

Figure 8. Trajectories with $\phi_1 = 0.4$, $\phi_2 = 0.3$ and $\theta = 0.2$ for $R_0 > 1$.

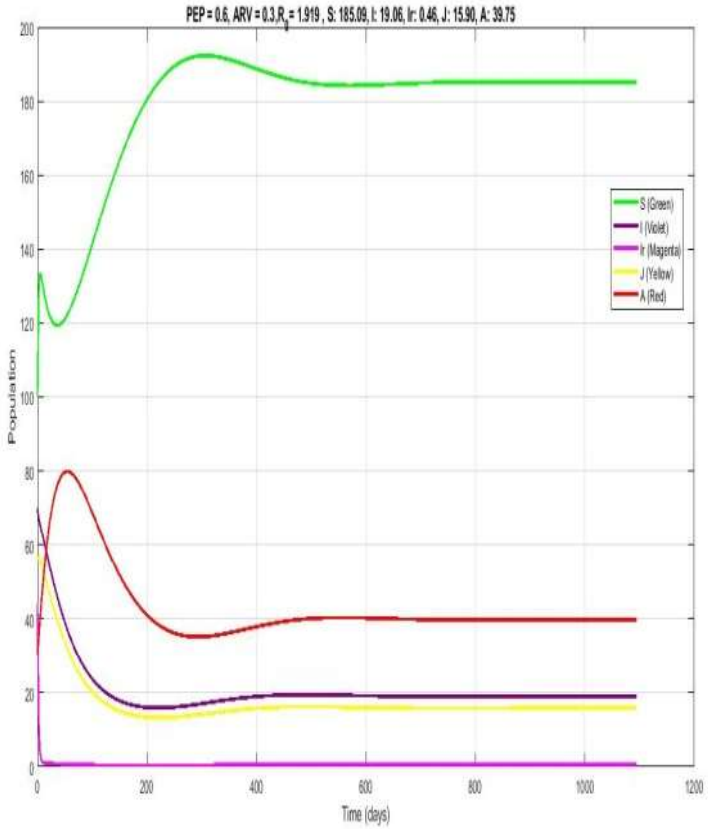

Figure 9. Trajectories with $\phi_1 = 0.6$, $\phi_2 = 0.3$ and $\theta = 0.2$ for $R_0 > 1$.

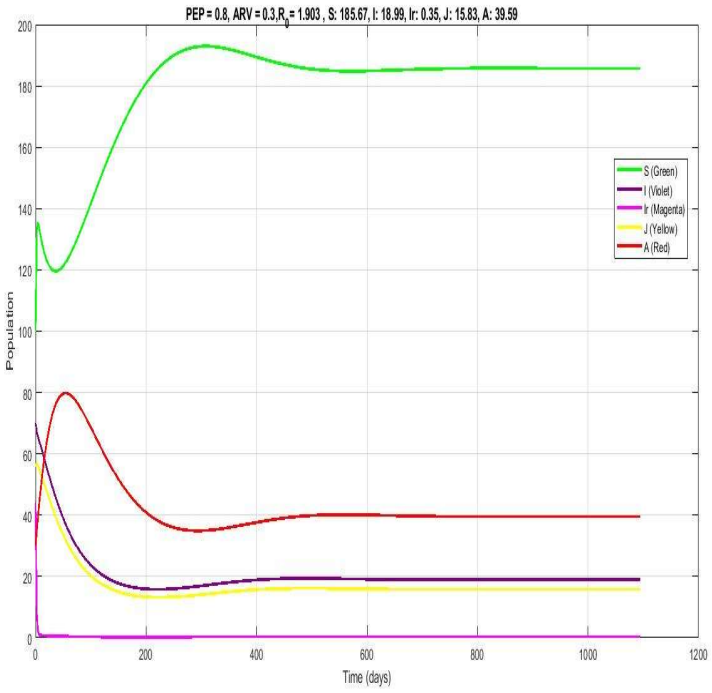

Figure 10. Trajectories with $\phi_1 = 0.8$, $\phi_2 = 0.3$ and $\theta = 0.2$ for $R_0 > 1$.

These trajectories in revealed that the susceptible population initially decreases and then starts to increase to the endemic equilibrium state. On the other hand, the infected compartments S, I, I_r, J and A gradually decline and stabilize at lower endemic levels with increasing time.

These results confirm that increase in PEP coverage facilitate curbing new HIV infections during or after recent possible exposure and hence significantly reduce the disease burden within a population. Endemic equilibrium points and R_0 are also computed at different PEP ($\emptyset_1$) treatment rates as summarized in **Table 5.**

Table 5. Equilibrium points at different values of $\emptyset_1$ and θ = 0.2.

PEP($\emptyset_1$)	**ARV($\emptyset_2$)**	**S**	**I**	**I_r**	**J**	**A**	**$R_0(\emptyset_1)$**
0.0	0.0	159.75	3.62	14.02	20.43	51.07	3.922
0.1	0.3	175.75	20.23	2.48	16.92	42.31	2.209
0.2	0.3	180.89	19.60	1.32	16.36	40.92	2.046
0.4	0.3	183.97	19.22	0.68	16.01	40.06	1.953
0.6	0.3	185.09	19.06	0.46	15.9	39.75	1.919
0.8	0.3	185.67	18.99	0.35	15.85	39.59	1.903

Our results in the table illustrate that whenever there is no treatment, the endemic equilibrium become stable at more endemic level compared with the endemic points in the presence of treatment; for example, compare the rows of the table. The table also illustrate that as the rate of PEP treatment increases from $\emptyset_1 = 0$ to $\emptyset_1 = 0.8$, the susceptible population S increase from 159.75 to 185.67 and the infected classes decreased from (I, I_r, J, A) decreases from (19.60, 1.32, 16.36, 40.92) to (18.99, 0.35, 15.85, 39.59) indicating the post exposure prophylaxis significantly ease the burden of the epidemic by decreasing the rape related new infections. In particular, the scenario of rape related HIV infection I_r against PEP treatment rate is very well observed in the table. The sub population Ir shows significant decrease in fact sharp decrease, from 14.02 at no PEP treatment $\emptyset_1 = 0$ to 2.48 at PEP rate $\emptyset_1 = 0.1$ and then gradually decreased to 0.35 when $\emptyset_1 = 0.8$. Furthermore, **Table 5** clearly demonstrate that the basic reproduction number R_0 decreasing from 3.922 in the absence of PEP to 1.903 at PEP rate $\emptyset_1 = 0.8$. This dynamic is particularly confirmed that lower PEP coverage significantly contributes to the force of infection.

The effect of combined variations in PEP($\emptyset_1$) coverage, ARV($\emptyset_2$) treatment rate, and rape prevalence (θ) on the reproduction number (R_0) is illustrated using simulation including surface and contour plots as shown from **Figure 11 to Figure 20**. These plots show how R_0 responds to changes in PEP and rape prevalence, ARV and rape prevalence, as well as the simultaneous variation of PEP, ARV, and rape prevalence.

The result of **Figure 11** and **Figure 12** demonstrates that the relationship between R_0 with PEP and ARV coverage. These figures show as PEP and ARV coverage decreases, R_0 increases which is a clear inverse relationship between the

coverage of PEP and ARV with R_0. **Figure 13** also indicates whenever the rape related infection rate increases the basic reproduction number increases linearly.

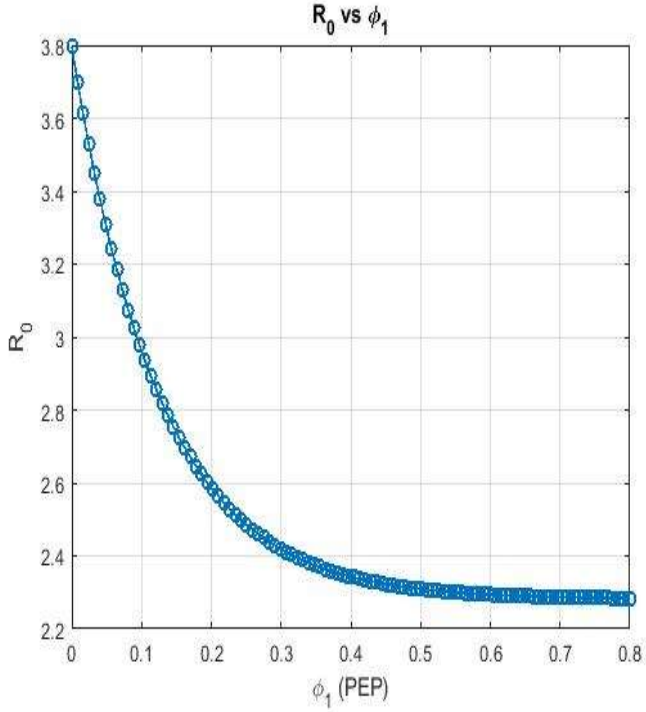

Figure 11. Effect of PEP rate (ϕ_1) on R_0

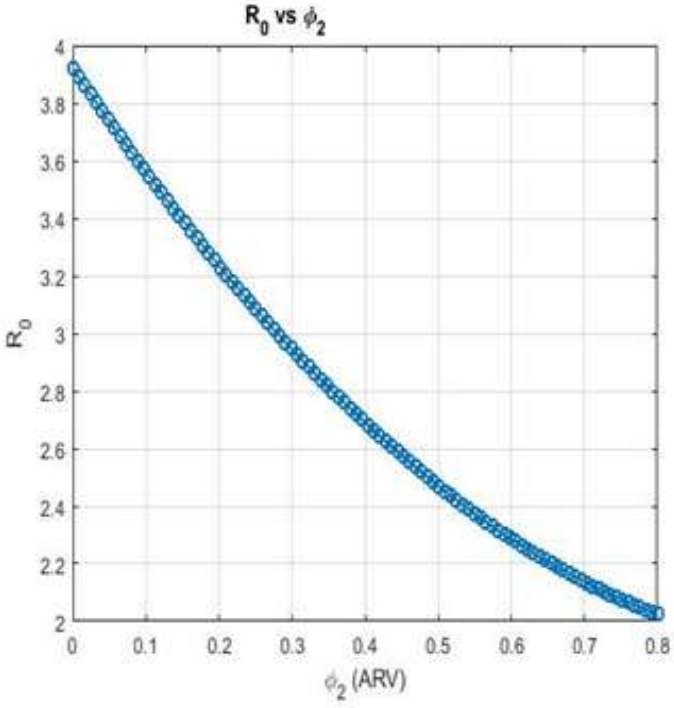

Figure 12. Effect of ARV rate (ϕ_2) on R_0

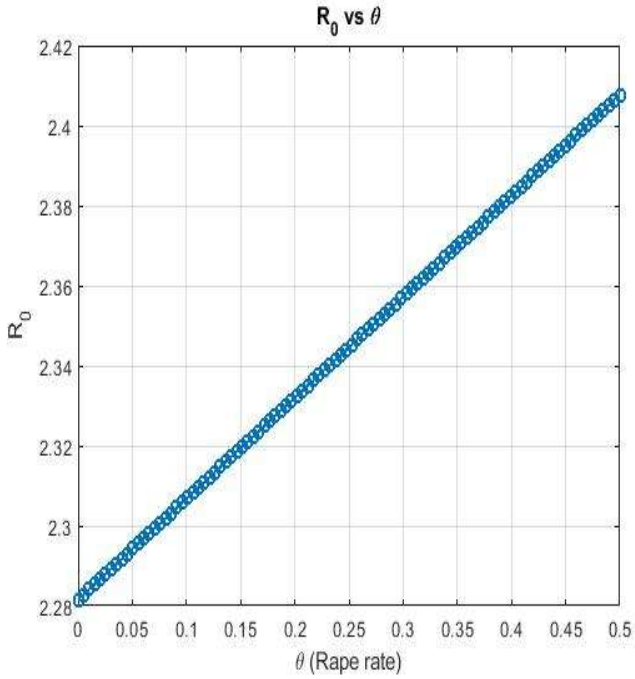

Figure 13. Effect of rape prevalence (θ) on R_0

The surface plots in **Figure 14** and **Figure 15** further illustrate the combined effects of PEP coverage and rape-related exposure rate, and ARV coverage and rape-related exposure rate, on R_0, respectively. These surface plots show that R_0 increases whenever PEP or ARV coverage decreases and rape-related infections rise. Notably, R_0 increases more sharply with decreasing ARV coverage than with decreasing PEP coverage, highlighting the stronger mitigating effect of PEP in reducing the transmission of HIV from rape-related exposures compared to ARV alone.

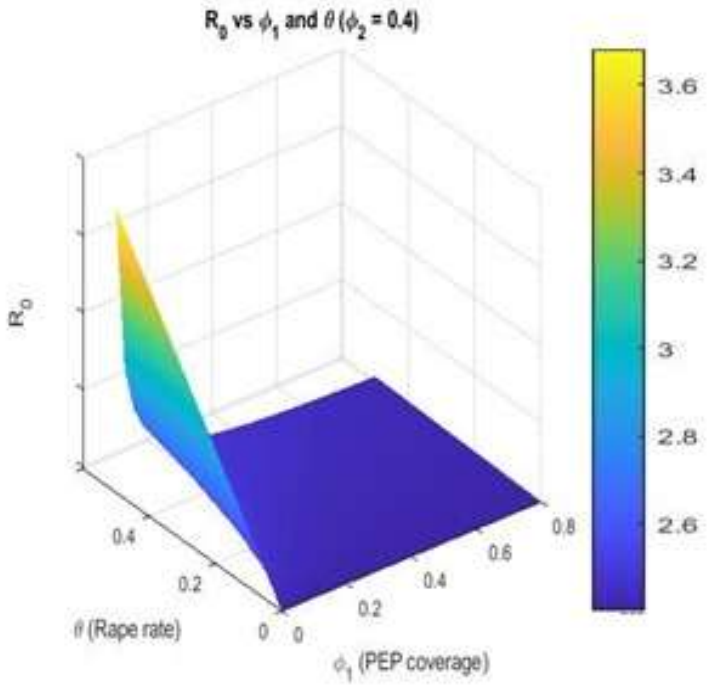

Figure 14. Effect of PEP rate (ϕ_1) and rape prevalence (θ) on R_0

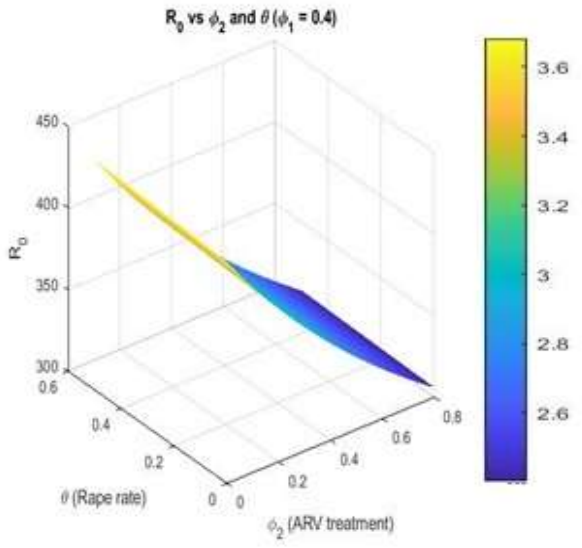

Figure 15. Effect of ARV rate (ϕ_2) and rape prevalence (θ) on R_0

How the rape related infections impact the HIV transmission dynamics were also examined through contour plots of R_0 against varying levels of PEP and ARV coverage under different rape prevalence scenarios ($\theta = 0.05,0.1,0.15,0.2,0.25$), as illustrated in **Figures 16–20**. These plots demonstrate that the basic reproduction number R_0 consistently increases as the prevalence of rape-related infection rises, even when PEP and ARV coverage are enhanced. This indicates that sexual violence remains a strong driver of HIV transmission, and that while treatment interventions can mitigate transmission, high rates of rape can substantially offset these gains. The analysis highlights the critical need for combined strategies that address both medical interventions and the prevention of sexual violence to effectively control HIV spread in conflict-affected settings.

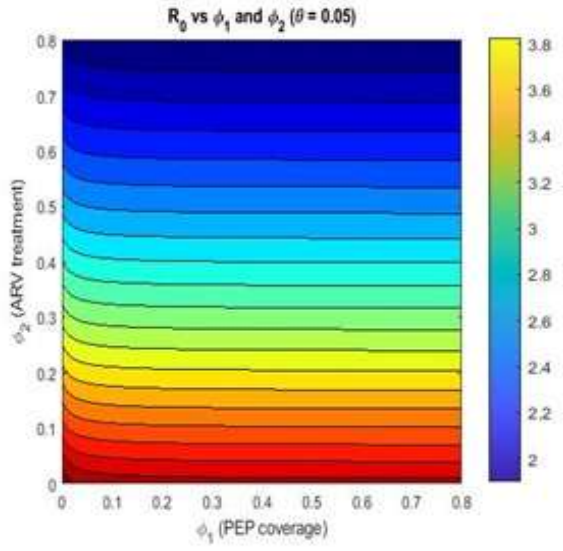

Figure 16. Effect of PEP (ϕ_1) and ARV (ϕ_2) rates on R_0

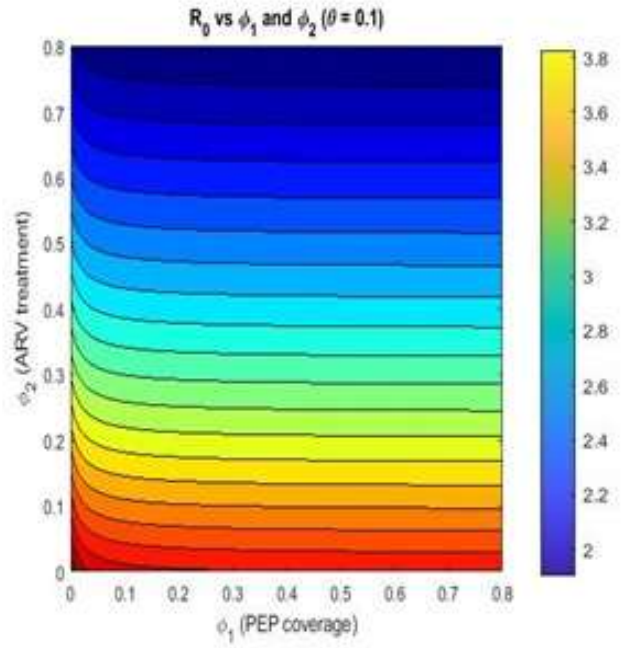

Figure 17. Effect of PEP (ϕ_1) and ARV (ϕ_2) rates on R_0

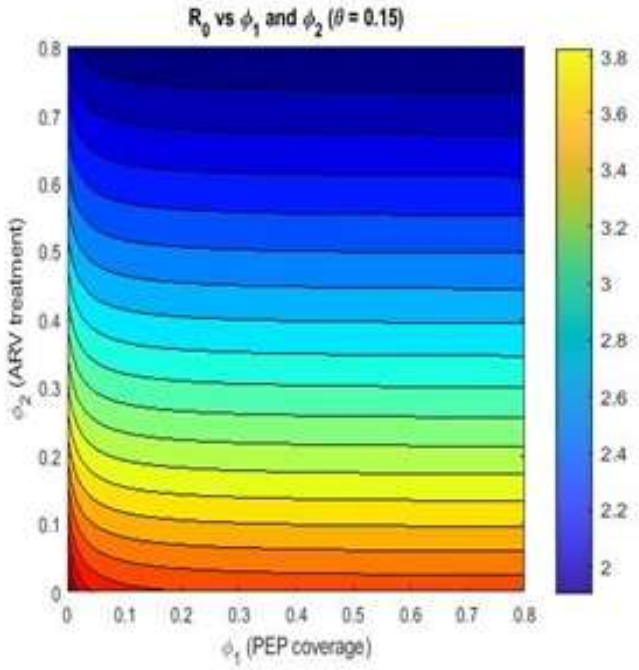

Figure 18. Effect of PEP (ϕ_1) and ARV (ϕ_2) rates on R_0

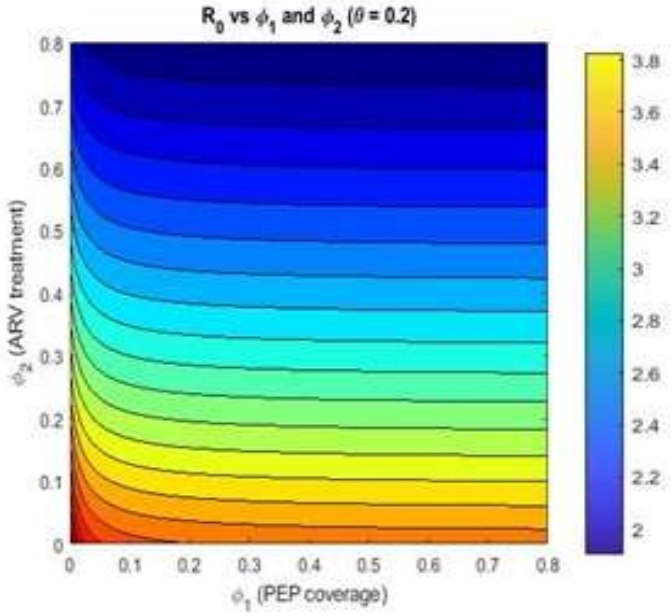

Figure 19. Effect of PEP (ϕ_1) and ARV (ϕ_2) rates on R_0.

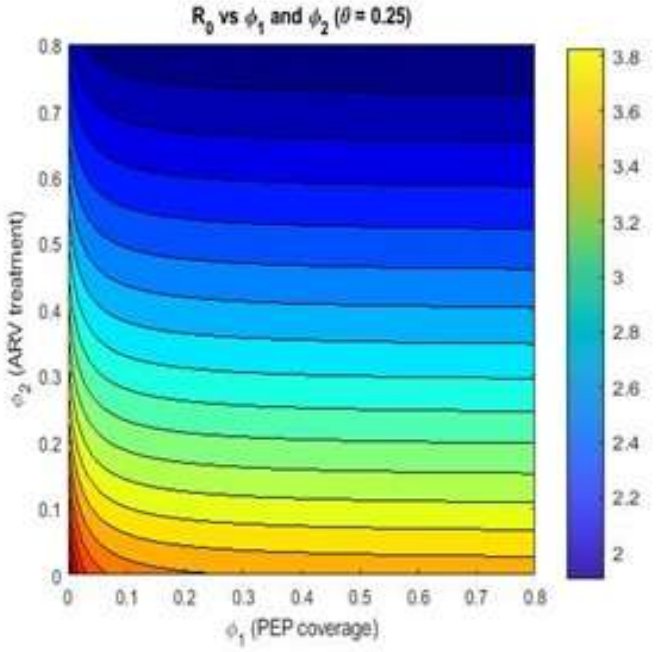

Figure 20. Effect of PEP (ϕ_1) and ARV (ϕ_2) rates on R_0.

Despite the significant impacts of treatments in curbing the disease, the trajectories of the infected classes are at non-zero endemic levels even with high PEP treatment rates. Furthermore, the values of R_0 of the model system (2) presented in **Table 5** remain greater than the threshold value ($R_0 = 1$), all of these indicating the stability of the disease at an endemic level. These results also imply the persistence of the disease in the population, and by which our analytical result of **Theorem 5**, "the endemic equilibrium point is globally asymptotically stable whenever $R_0 > 1$",

is validated; this is, in fact, consistent with both biological plausibility and empirical findings.

In general, the outcomes of this study signify the critical role of treatments. It underlines those reductions in PEP coverage substantially increase the basic reproduction number R_0, facilitating the persistence and expansion of the HIV virus. It also demonstrates that in the presence of rape-related HIV infection, the disease remains endemic even under high PEP treatment coverage for $R_0 > 1$, emphasizing the persistence of the virus in the population. This study, therefore, carries significant public health implications for HIV control, particularly in humanitarian crises, including conflict-affected regions where health systems are devastated and sexual violence is prevalent.

Thus, maintaining or restoring access to PEP and ARVs in humanitarian crises is essential not only for individual care but also to prevent escalation of the epidemic to endemic proportions. Our study results advocate for the rapid deployment of PEP kits, training of frontline health workers, and community sensitization to interrupt viral replication before systemic infection occurs. International agencies, donors, and governments must ensure continuity of HIV treatment services even during active conflict through mobile clinics, cross-border care, and community health workers to mitigate long-term epidemiological consequences.

7. Conclusion

In this paper, we investigated an HIV/AIDS transmission dynamics model that explicitly incorporates rape-related transmission and the mitigating effects of PEP and ARV treatment. We established the existence, uniqueness, and positivity of solutions, and analyzed the basic reproduction number (R_0). Through this analysis, we proved the global stability of both the disease-free and endemic equilibrium points. Specifically, the disease-free equilibrium is globally asymptotically stable when $R_0 < 1$, indicating that the disease can be eliminated from the population. Conversely, when $R_0 > 1$, the endemic equilibrium becomes globally stable and the infection persists at a steady level in the population. Numerical simulations were conducted to explore the dynamics of HIV transmission under different levels of PEP and ARV treatment. The results show that both interventions significantly reduce HIV incidence, with higher coverage leading to faster disease elimination when $R_0 < 1$, and to lower endemic levels when $R_0 > 1$. Without treatment, the disease stabilizes at a higher endemic state. The study also underscores the importance of timely administration of PEP, ideally within 72 hours of exposure, as recommended by the World Health Organization. This has critical public health implications, particularly for the tens of thousands of women and girls at risk of rape-related HIV infection in conflict-affected regions. Our findings call for urgent action from governments, United Nations agencies, and non-governmental organizations to develop and implement comprehensive HIV prevention and treatment strategies. These efforts should prioritize high-risk populations, with a focus on survivors of SGBV and mass rape in humanitarian emergencies.

Author contributions: Conceptualization, AMM, HAA, YYK, KTG and WAW;

methodology, AMM, HAA, YYK, KTG and WAW; software, AMM, HAA, YYK, KTG and WAW; validation, AMM, HAA, YYK, KTG and WAW; formal analysis, AMM, HAA, YYK, KTG and WAW; investigation, AMM, HAA, YYK, KTG and WAW; writing, original draft preparation, AMM, HAA, YYK, KTG and WAW; writing, review and editing, AMM, HAA, YYK, KTG and WAW; visualization, AMM, HAA, YYK, KTG and WAW; supervision, HAA, YYK, KTG and WAW; project administration, HAA, YYK, KTG and WAW. All authors have read and agreed to the published version of the manuscript.

Funding: There is no financial support for this work. All the authors declare that no funding was used.

Conflict of interest: The authors declare that they have no competing interests with this publication.

Ethical statement: The research was carried out by complying with national and international scientific and ethical guidelines. The research protocol was reviewed by the Institutional review Board of Mekelle University, College of Health Science and Ayder Comprehensive Specialized Hospital and has received expedited approval on 11 April 2024.

Data availability statement: All datasets generated and/or analyzed during the current study are publicly available.

References

1. Daw MA, El-Bouzedi HA, Ahmed MO. The impact of armed conflict on the prevalence and transmission dynamics of HIV infection in Libya. Front Public Health. 2022; 10: 779778. doi: 10.3389/fpubh.2022.779778
2. Kebede HK, Gesesew H, Ward P. Impact of armed conflicts on HIV treatment outcomes in sub-Saharan Africa: protocol for a systematic review and meta-analysis. BMJ Open. 2023; 13: e069308. doi: 10.1136/bmjopen-2022-069308
3. UNAIDS. Global HIV & AIDS Statistics – fact sheet. Available online: https://www.unaids.org/en/resources/fact-sheet (accessed on 2 June 2025).
4. UNESCO. International Technical Guidance on Sexuality Education: An Evidence-informed Approach. Revised ed. UNESCO, UNAIDS, UNFPA, UNICEF, UN Women & WHO; 2018. Available online: https://cdn.who.int/media/docs/default-source/reproductive-health/sexual-health/international-technical-guidance-on-sexuality-education.pdf (accessed on 2 June 2025).
5. United Nations Security Council. Resolution: Women and Peace and Security. United Nations; 2008. Available online: https://undocs.org/S/RES/1820(2008) (accessed on 2 June 2025).
6. Carpio MA. In the Democratic Republic of Congo, the double punishment of raped women (France). Available online: https://www.nationalgeographic.fr/histoire/en-republique-democratique-du-congo-la-double-peine-des-femmes-violees (accessed on 2 June 2025).
7. Anema A, Joffres MR, Mills E, Spigel PB. Widespread rape does not directly appear to increase the overall HIV prevalence in conflict-affected countries: so now what? Emerging Themes in Epidemiology. 2008; 5: 11. doi: 10.1186/1742-7622-5-11
8. Supervie V, Halima Y, Blower S. Assessing the impact of mass rape on the incidence of HIV in conflict-affected countries. AIDS. 2010; 24(18): 2841–2847. doi: 10.1097/QAD.0b013e32833fed78
9. Fisseha G, Gebrehiwot TG, Gebremichael MW, et al. War related sexual and gender-based violence in Tigray, Northern Ethiopia: a community-based study. BMJ Global Health. 2023; 8(7): e010270. doi: 10.1136/bmjgh-2022-010270
10. Abrahams N, Mhlongo S, Dunkle K, et al. Increase in HIV incidence in women exposed to rape. AIDS. 2021; 35(4): 633–642. doi: 10.1097/QAD.0000000000002779
11. Mootz JJ, Odejimi OA, Bhattacharya A, et al. Transactional sex work and HIV among women in conflict-affected Northeastern Uganda: a population-based study. Conflict and Health. 2022; 16: 8. doi: 10.1186/s13031-022-00441-5

12. Bennett BW, Marshall BDL, Gjelsvik A, et al. HIV incidence prior to, during, and after violent conflict in 36 Sub-Saharan African nations, 1990–2012: an ecological study. PLoS One. 2015; 10(11): e0142343. doi: 10.1371/journal.pone.0142343
13. Ba AT. Armed Conflicts, HIV Testing, HIV Prevalence, and High-Risk Sexual Behaviors: An Epidemiologic Analysis [PhD thesis]. Medical University of South Carolina; 2022. Available online: https://medica-musc.researchcommons.org/theses/704/ (accessed on 2 June 2025).
14. Ciswaka H, Oduoye MO, Masimango G, et al. Prevention and elimination efforts of HIV/AIDS caused by sexual violence against women in the Democratic Republic of the Congo: An editorial. International Journal of Gynecology & Obstetrics. 2024; 164(2): 385–386. doi: 10.1002/ijgo.15128
15. World Health Organization. WHO expands recommendation on oral pre-exposure prophylaxis of HIV infection (PrEP); 2015. Available online: https://www.paho.org/en/node/69890 (accessed on 2 June 2025).
16. Indonesian Ministry of Health. Consolidated Guidelines on the Use of Antiretroviral Drugs for Treating and Preventing HIV Infection (SIHA),2024. Available online: https://siha.kemkes.go.id/portal/files_upload/9789241549684_eng.pdf (accessed on 2 June 2025).
17. Nsuami MUN, Witbooi PJ. A stochastic model for HIV with the use of PrEP. Journal of Mathematical Modeling. 2021; 9(4): 537–553. doi: 10.22124/jmm.2021.16870.1461
18. Peter OJ, Abidemi A, Fatmawati F, et al. Optimizing tuberculosis control: a comprehensive simulation of integrated interventions using a mathematical model. Mathematical Modelling and Numerical Simulation with Applications. 2024; 4(3): 238–255. doi: 10.53391/mmnsa.1461011
19. Ulfa B, Trisilowati T, WM K. Dynamical analysis of HIV/AIDS epidemic model with treatment. The Journal of Experimental Life Science. 2018; 8(1): 23–29. doi: 10.21776/ub.jels.2018.008.01.04
20. Ouaziz SI, El Khomssi M. Mathematical approaches to controlling COVID-19: optimal control and financial benefits. Mathematical Modelling and Numerical Simulation with Applications. 2024; 4(1): 1–36. doi: 10.53391/mmnsa.1373093
21. Cai L, Li X, Ghosh M, Guo B. Stability analysis of an HIV/AIDS epidemic model with treatment. Journal of Computational and Applied Mathematics. 2009; 229(1): 313–323. doi: 10.1016/j.cam.2008.10.067
22. Bashiru KA, Ojurongbe TA, Kolawole MK, et al. Stability analysis of HIV/AIDS epidemic model in the presence of vertical transmission and treatment. UNIOSUN Journal of Engineering and Environmental Sciences. 2023; 5(1). doi: 10.36108/ujees/3202.50.0141
23. Turan M, Sevinik Adıguzel R, Koc F. Stability analysis of an epidemic model with vaccination and time delay. Mathematical Methods in the Applied Sciences. 2023; 46(14): 14828–14840. doi: 10.1002/mma.9348
24. Kasia Ayele T, Doungmo Goufo EF, Mugisha S. Mathematical modeling of HIV/AIDS with optimal control: A case study in Ethiopia. Results in Physics. 2021; 26: 104263. doi: 10.1016/j.rinp.2021.104263
25. Mustapha UT, Ado A, Yusuf A, et al. Mathematical dynamics for HIV infections with public awareness and viral load detectability. Mathematical Modelling and Numerical Simulation with Applications. 2023; 3(3): 256–280. doi: 10.53391/mmnsa.1349472
26. Baba IA, Yusuf A, Al-Shomrani M. A mathematical model for studying rape and its possible mode of control. Results in Physics. 2021; 22: 103917. doi: 10.1016/j.rinp.2021.103917
27. Islam KN, Biswas MHA. Mathematical Assessment for the Dynamical Model of Sexual Violence of Women in Bangladesh. In: Proceedings of the International Conference on Industrial & Mechanical Engineering and Operations Management; 26-27 December 2020; Dhaka, Bangladesh.
28. Gurmu ED, Bole BK, Koya PR. Mathematical modelling of HIV/AIDS transmission dynamics with drug resistance compartment. American Journal of Applied Mathematics. 2020; 8(1): 34–45. doi: 10.11648/j.ajam.20200801.16
29. Van den Driessche P, Watmough J. Reproduction numbers and subthreshold endemic equilibria for compartmental models of disease transmission. Mathematical Biosciences. 2002; 180(1–2): 29–48. doi: 10.1016/S0025-5564(02)00108-6
30. Lu G, Dou L, Miao Y, Chen L. Co-dynamics of measles and hand-foot-mouth disease: Reproduction number and equilibrium analysis. Mathematics and Systems Science. 2025; 3(2): 1–20. doi: 10.54517/mss3359
31. Berman A, Plemmons RJ. Nonnegative Matrices in the Mathematical Sciences. SIAM; 1994. doi:10.1137/1.9781611971262